Manuscript submitted to: Volume 2, Issue 1, 1-15.

AIMS Materials Science DOI: 10.3934/matersci.2015.1.1

Received date 8 December 2014, Accepted date 20 January 2015, Published date 30 January 2015

Research Article

The influence of organic structure and rare earth metal cation on the corrosion efficiency observed on AS1020 steel compared with $La(4OHCin)_3$

Marianne Seter [1], Gaetan M. A. Girard [1], Winnie W. Lee [2], Glen Deacon [2], Peter Junk [2,3], Bruce Hinton [1] and Maria Forsyth [1,*]

[1] ARC Centre of Excellence for Electromaterials Science, Institute for Frontier Materials, Deakin University, Burwood Campus, Australia

[2] Centre for Green Chemistry and School of Chemistry, Monash University, Clayton Campus, Australia

[3] College of Science, Technology, and Engineering, James Cook University, Townsville, Queensland, Australia

* **Correspondence:** Email: mf-research@deakin.edu.au.

Abstract: Whilst the corrosion protection of steel in aqueous chloride environments by the rare earth inhibitor lanthanum 4-hydroxycinnamate is well known, the influence of the structural variation of the organic component as well as the nature of the metal centre has not previously been addressed. Herein we show that praseodymium 4-hydroxy cinnamate is comparable to its lanthanum counterpart in aqueous solution. On the other hand, cerium 4-hydroxycinnamate and lanthanum 2-hydroxycinnamate show poor corrosion protection performance while lanthanum 3-hydroxycinnamate provides a level of inhibition between these. These differences are shown to be related to the speciation in solution and are postulated to be linked to steric influences which are likely to affect the bonding environment within the rare earth compound itself, as well as its bonding with the steel substrate.

Keywords: corrosion inhibition; rare earth metal compounds; cinnamates; speciation

1. Introduction

In order to ameliorate the deterioration of metal substrates from the effects of harsh environments, environmentally friendly inhibitors are an ideal alternative to the carcinogenic and

toxic chromates [1−4]. Such inhibitors are able to reinforce the metal oxide film or alternatively deposit complexes onto the metal substrate [4,5,6]. There is an increased demand for more environmentally friendly and cost effective protection against corrosion; such alternatives include inorganic compounds, e.g. nitrates, molybdates, and rare earths, and organic compounds such as carboxylates, phosphonates, phosphates and sulphonates [7,8,9]. Over the past decade Forsyth and co-workers have developed a range of rare earth organic compounds that show promise as environmentally friendly corrosion inhibitors for steel substrates, in particular lanthanum 4-hydroxycinnamate [10−16].

Recently, lanthanum 4-hydroxycinnamate in solution has shown remarkable corrosion inhibition properties with mild steel substrates [15]. This compound performs better as an inhibitor of steel at higher concentrations and under alkaline conditions. Under acidic pH conditions dissociation of the lanthanum 4-hydroxycinnamate, ($La(4OHCin)_3$, occurs where the predominant species are lanthanum chloride $[LaCl_4]^-$ and 4-hydroxylcinnamic acid as separate entities in solution. This leads to a rather low mixed inhibition effect compared with the strong anodic inhibition observed at higher pH values when the complex $[LaL_4]^-$ is present [15]. The observation that slight cathodic inhibition was more evident under acidic conditions (except for high concentrations, i.e 1000 ppm where the inhibition was via both anodic and cathodic processes), and that this correlated with an excess of the $LaCl_4^-$ species, strongly suggests that the speciation of $La(4OHCin)_3$ is critical to the anodic nature and high efficiency of the inhibition and confirms the synergy of the organic and REM components previously suggested by Forsyth et al. [17].

It was certainly interesting to discover that this inhibitor might be capable of functioning well over a wide pH range, and that the inhibition mechanism could also vary over that range.

The study of the speciation for $La(4OHCin)_3$ and its influence on the corrosion inhibition efficiency for steel substrates over a wide range of environmental conditions has provided an in depth perception of the working mechanism of the inhibitor. The aim of this current work was to investigate the influence of the position of substitution of the aromatic ring of the organic component of the inhibitor, and the influence of the rare earth metal coordinated by the cinnamate ion. This included analysis of lanthanum 2-hydroxycinnamate ($La(2OHCin)_3$), lanthanum 3-hydroxycinnamate ($La(3OHCin)_3$), praseodymium 4-hydroxycinnamate ($Pr(4OHCin)_3$) and cerium 4-hydroxycinnamate ($Ce(4OHCin)_3$). These studies could lead to more clever choices of inhibitor combinations, and a better understanding of the influence of chemical structure and bonding which could allow design of improved inhibition properties for this type of inhibitor compound.

2. Materials and Method

2.1. Chemicals and Materials

The x-hydroxy cinnamic acid, where x is 2, 3 and 4, and the lanthanum, praseodymium, and cerium chlorides were purchased from Sigma Aldrich. The rare earth 4-hydroxycinnamates were prepared according to already published methodology [18] while the $La(2OHCin)_3$ and $La(3OHCin)_3$ were prepared by similar metathesis synthesis between the corresponding sodium salts and lanthanum chloride, refer to Electronic Supplementary Information (ESI) for experimental details, including the powder X-ray diffraction pattern for $La(3OHCin)_3$. All test solutions were prepared using reagent grade sodium chloride (Chem Supply), sodium hydroxide (Merck) and hydrochloric acid (Merck)

solutions. The use of deionised water for the preparation of all solutions was adopted. The working electrodes used for the potentiodynamic polarisation experiments were machined from a cylindrical mild steel rod, Australian standard AS1020, to a 1.0 cm diameter (0.78 cm^2). These electrodes were coated with an epoxy resin and attached to a teflon holder. The steel coupons used for the constant immersion corrosion tests were prepared also from a 2.0 cm diameter mild steel rod, AS1020, to a thickness of 0.3 cm.

2.2. Electrode and Coupon Preparation

The working electrodes for use in the potentiodynamic polarisation studies and the corrosion test coupons were abraded with silicon carbide paper to a P4000 grit finish from P320 grit. They were washed with tap water followed by DI water, and dried using nitrogen gas. Potentiodynamic polarisation and corrosion tests were carried out immediately after specimen preparation, which aided reproducibility.

The test solutions were prepared by dissolving the appropriate weights of each rare earth x-hydroxy cinnamate in 1 L to make concentrations of 400 and 600 ppm in 0.01 M sodium chloride solution. The pH of the solutions was adjusted using 0.01 M hydrochloric acid solution to achieve pH 2.5. The unadjusted pH of the prepared solution was pH 5.5. The solutions were exposed to a temperature-controlled laboratory atmosphere at approximately 22 °C.

2.3. Potentiodynamic Polarisation

Using potentiodynamic polarization experiments it is possible to determine the inhibitive nature of the rare earth cinnamates at different concentrations and solution pH in an open-to-air environment.

All polarisation experiments were carried out open-to-air using 100 mL of inhibitor solution in a standard three-electrode system consisting of a saturated calomel reference electrode, a titanium mesh counter electrode, and the working electrode. The cell assembly was located in a Faraday cage to prevent electrical interference. The exposed area of the working electrode was 0.78 cm^2. After immersion the open circuit potential (OCP) was monitored for 12 hours, and then the potentiodynamic polarisation experiment was carried out at a scanning rate of 0.1667 mV s^{-1}. The scans started at 200 mV more negative than E_{corr} and continued through E_{corr} for a range of 1.0 V in the positive direction. Polarisation curves were replicated in triplicate to assess reproducibility. All electrochemical measurements were conducted using a Biologic VMP multichannel potentiostat with EC-Lab v 10.32 software used for analysis. The current density (i_{corr}) values were calculated using Tafel extrapolation methods. Where anodic and cathodic curves were near linear and symmetrical within +/− 50 mV from E_{corr}, both Tafel slopes were extrapolated until the lines intersected at E_{corr}. Where polarisation occurred for the cathodic reaction under acidic conditions, the slope for the cathodic region was extrapolated until it intersected the E_{corr} value.

2.4. Nuclear Magnetic Resonance Spectroscopy (NMR)

A Jeol 270 MHz spectrometer was used to collect ^{139}La (38.2 MHz) NMR spectra. A double pulse spin echo experiment was used with a 180° pulse duration of 26.4 μs followed by a 90° pulse duration of 13.2 μs. Spectra were collected using 4096 transients, a 0.36 s acquisition time, and a 0.30 s

relaxation delay. Each spectrum had the subsequent processing parameters applied using MestReNova 7.0.3: smoothing via Whittaker Smoother method, phase correction, and baseline correction. Peak widths at half height were measured. All NMR spectra are reported as their corresponding chemical shifts δ. A solution of 0.01 M lanthanum chloride in D_2O was used as an external standard to reference the ^{139}La chemical shifts.

NMR experiments were run at room temperature in 10 mm NMR tubes for the 400 ppm lanthanum x-hydroxycinnamate solutions at pH 5.5.

2.5. Electrospray Mass Spectroscopy (ESMS)

An Agilent Technologies LC/MSD TOF with acetonitrile as the mobile phase with a flow rate of 25 μL min^{-1} was used to collect mass spectrometry data. All inhibitor solutions were directly injected into the spectrometer, with nitrogen gas used for nebulisation. Data were collected using Agilent MassHunter Workstation Data Acquisition software and analysed using Agilent MassHunter Qualitative Analysis software.

3. Results and Discussion

3.1. Anodic polarisation of steel in inhibitor solutions

Typical potentiodynamic polarisation curves for the inhibitors at 400 ppm and 600 ppm at pH 2.5 and 5.5 revealed that they all suppressed the anodic reaction to some degree (Figures 1–4). At these concentrations for pH 2.5, only a slight shift of E_{corr} was observed toward more noble potentials, except for $La(2OHcin)_3$ which showed a slight cathodic shift in the potential. This is most likely due to the dissociation of the inhibitor into its rare earth chloride and cinnamate ions, a similar trend was seen in previous work for $La(4OHCin)_3$ at pH 2.5 [15]. According to Table 1 and 3, E_{corr} and I_{corr} values calculated from the potentiodynamic polarisation curves for the inhibitors at concentrations of 400 and 600 ppm and pH 2.5 show that $La(4OHCin)_3$ was by far the best inhibitor under these conditions with I_{corr} being reduced compared to control solution values (Figure 1). Interestingly, the $Pr(4OHCin)_3$ and $La(3OHCin)_3$ showed comparable behaviour, to the results for the $La(4OHCin)_3$. In contrast however, the E_{corr} and I_{corr} values calculated for the $La(2OHCin)_3$ and $Ce(4OHCin)_3$ are very poor, being almost the same as for the control solution values.

Increasing the pH of the inhibitor solution to pH 5.5 gave a much clearer indication of the trend seen from the potentiodynamic polarisation curves found at pH 2.5, suggesting that the $Pr(4OHCin)_3$ and $La(3OHCin)_3$ were almost as efficient as the $La(4OHCin)_3$ (Figure 2 and 4). This is supported by the Tafel extrapolation data collected at both concentrations, as presented in Table 2 and 4.

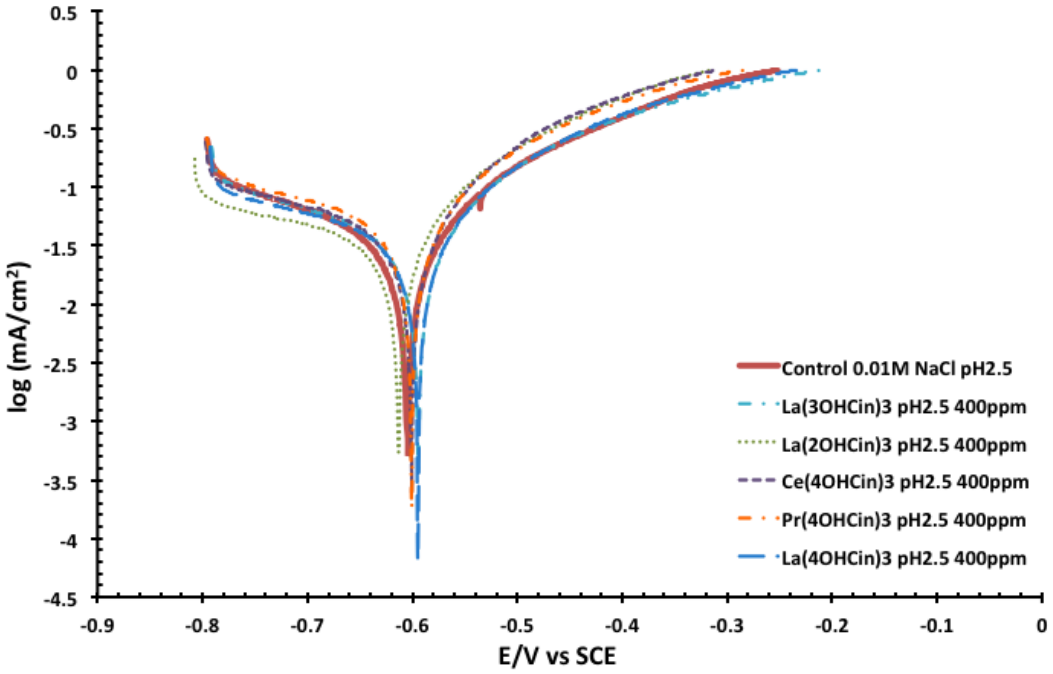

Figure 1. Potentiodynamic polarisation curves for rare earth cinnamates in 0.01 M NaCl solution at 400 ppm and pH 2.5. Polarisation curves are compared to a control experiment consisting of 0.01M NaCl solution at pH 2.5.

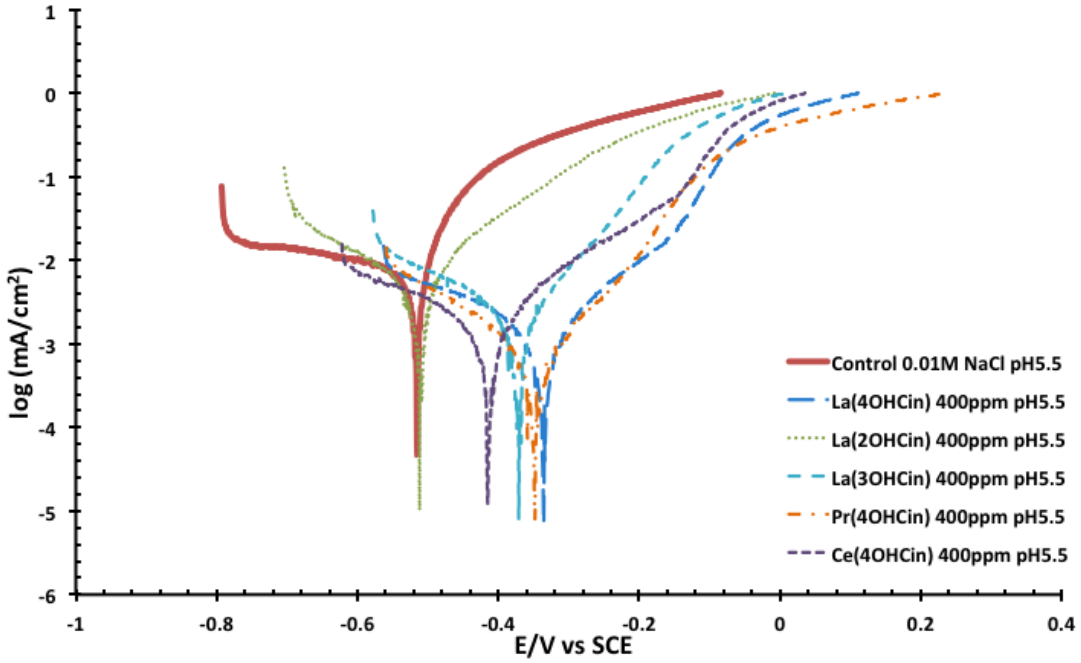

Figure 2. Potentiodynamic polarisation curves for rare earth cinnamates in a 0.01M NaCl solution at 400 ppm and pH 5.5. Polarisation curves are compared to a control experiment consisting of 0.01M NaCl solution at pH 5.5.

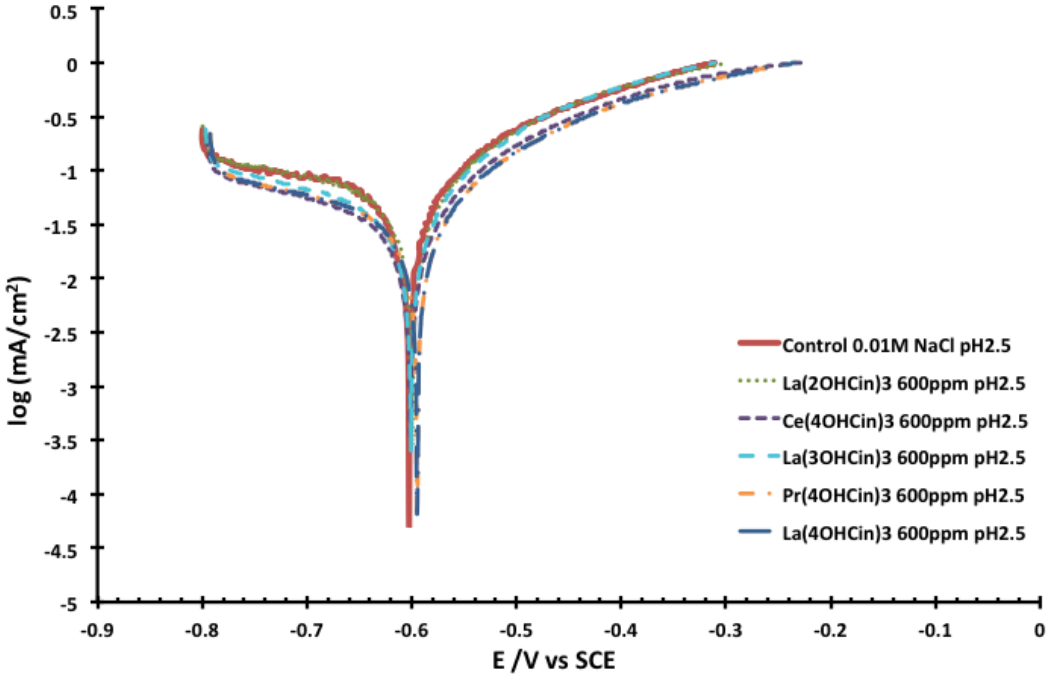

Figure 3. Potentiodynamic polarisation curves for rare earth cinnamates in a 0.01M NaCl solution at 600 ppm and pH 2.5. Polarisation curves are compared to a control experiment consisting of 0.01M NaCl solution at pH 2.5.

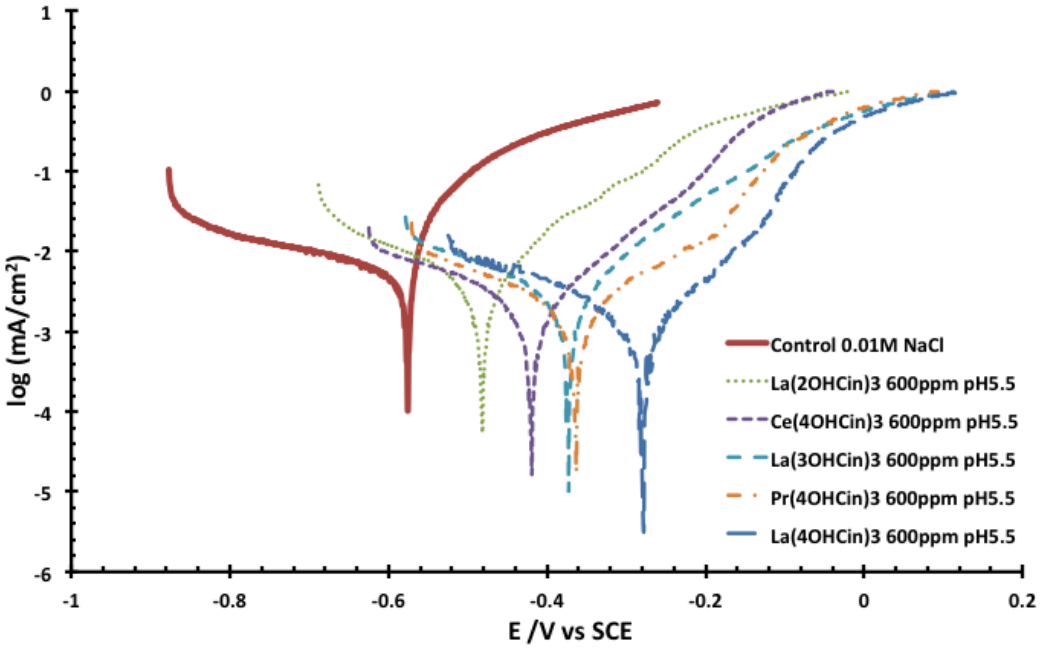

Figure 4. Potentiodynamic polarisation curves for rare earth cinnamates in a 0.01M NaCl solution at 600 ppm and pH 5.5. Polarisation curves are compared to a control experiment consisting of 0.01M NaCl solution at pH 5.5.

Table 1. Corrosion potential, E_{corr}, and corrosion current, I_{corr}, extracted from PP measurements (Tafel extrapolation) for at solution of 400 ppm RE Cinnamates at pH 2.5.

	I_{corr} ($\mu A/cm^2$)				
Solution	***1***	***2***	***3***	**Av. I_{corr}**	**E_{corr}**
0.01M NaCl	8.8	7.9	8.8	8.5	-603
$La(2OHCin)_3$	11.2	11.5	-	11.4	-614
$Ce(4OHCin)_3$	9.0	9.3	9.1	9.2	-601
$La(3OHCin)_3$	5.2	5.7	4.9	5.3	-601
$Pr(4OHCin)_3$	9.2	8.8	8.9	9.0	-601
$La(4OHCin)_3$	4.5	4.3	-	4.4	-599

Table 2. Corrosion potential, E_{corr}, and corrosion current, I_{corr}, extracted from PP measurements (Tafel extrapolation) for at solution of 400 ppm RE Cinnamates at pH 5.5.

	I_{corr} ($\mu A/cm^2$)				
Solution	***1***	***2***	***3***	**Av. I_{corr}**	**E_{corr}**
0.01M NaCl	2.1	2.1	-	2.1	-515
$La(2OHCin)_3$	2.3	2.3	2.1	2.2	-512
$Ce(4OHCin)_3$	1.9	1.9	1.8	1.9	-415
$La(3OHCin)_3$	0.6	0.6	0.6	0.6	-371
$Pr(4OHCin)_3$	0.4	0.4	0.4	0.4	-348
$La(4OHCin)_3$	0.3	0.3	-	0.3	-336

Table 3. Corrosion potential, E_{corr}, and corrosion current, I_{corr}, extracted from PP measurements (Tafel extrapolation) for at solution of 600 ppm RE Cinnamates at pH 2.5.

	I_{corr} ($\mu A/cm^2$)				
Solution	***1***	***2***	***3***	**Av. I_{corr}**	**E_{corr}**
0.01M NaCl	8.8	7.9	8.8	8.5	-603
$La(2OHCin)_3$	10.7	10.9	-	10.8	-603
$Ce(4OHCin)_3$	9.9	10.2	9.9	10.0	-601
$La(3OHCin)_3$	5.5	5.9	5.2	5.6	-601
$Pr(4OHCin)_3$	4.1	4.1	-	4.1	-594
$La(4OHCin)_3$	1.8	2.1	2.1	2.0	-595

Table 4. Corrosion potential, E_{corr}, and corrosion current, I_{corr}, extracted from PP measurements (Tafel extrapolation) for at solution of 600 ppm RE Cinnamates at pH 5.5.

	I_{corr} ($\mu A/cm^2$)				
Solution	***1***	***2***	***3***	**Av. I_{corr}**	**E_{corr}**
0.01M NaCl	2.1	2.1	-	2.1	-515
$La(2OHCin)_3$	1.3	1.3	1.3	1.3	-481
$Ce(4OHCin)_3$	0.5	0.4	-	0.5	-419
$La(3OHCin)_3$	0.4	0.4	0.4	0.4	-372
$Pr(4OHCin)_3$	0.3	0.3	0.3	0.2	-363
$La(4OHCin)_3$	0.7	0.6	0.6	0.6	-278

3.2. Characterisation of species in inhibitor solutions

Previous work has shown that the use of NMR spectroscopy in combination with electrospray mass spectrometry gives valuable information about the species present in solution in a given environment [15].

NMR is a powerful chemical characterisation tool and has been used to evaluate the change in solution speciation of the $La(4OHCin)_3$ under various pH and concentration conditions [15].

However, NMR spectroscopy has limitations in that it can only analyse NMR active nuclei, therefore in this case only the lanthanum species can be evaluated as the cerium and praseodymium nuclei are not active [19]. A spectrum of lanthanum chloride in D_2O was used as a reference where the signal resonates at δ 4.89 ppm. From Figure 5 it can be seen that there was a clear shift to higher resonances as the position of the hydroxyl group was changed from 4-hydroxy- to 3-hydroxy- and then the 2-hydroxycinnamate respectively.

Previous work has shown that an increase in concentration of the $La(4OHCin)_3$ at any given pH results in a shift to higher frequencies and increases the broadness of the peak [15]. It was concluded from the speciation study of the $La(4OHCin)_3$ that a shift to higher frequencies and increasing broadness were an indication of the presence of a number of different species in solution, and that the exchange between the species could lead to short relaxation times (T2) and lifetime broadening [20,21].

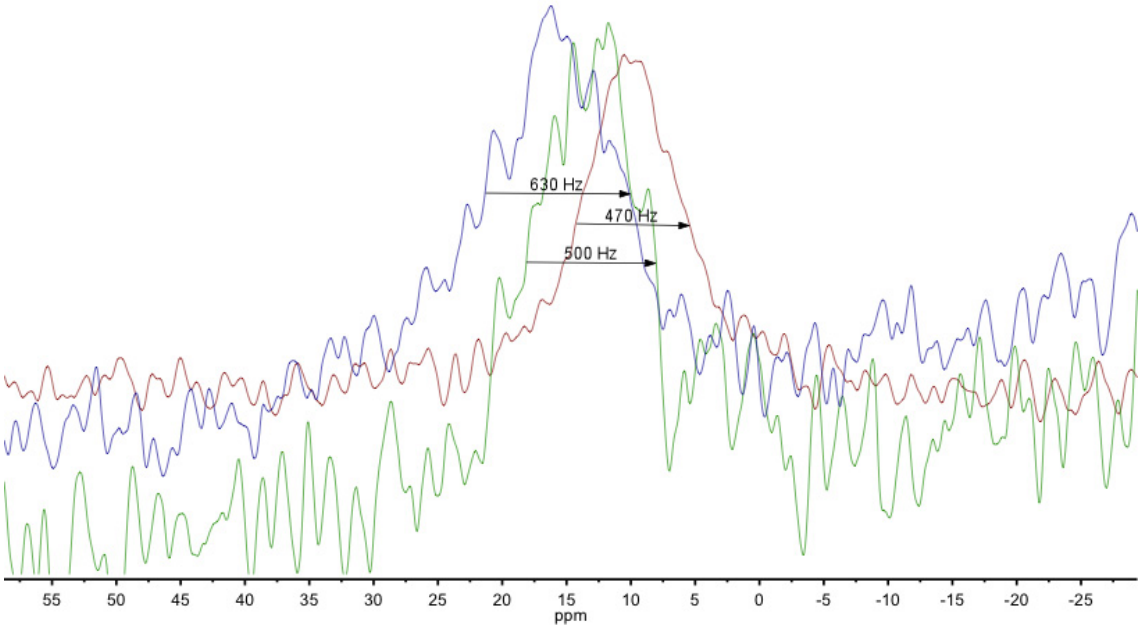

Figure 5. ^{139}La NMR spectra of lanthanum 2-hydroxy cinnamate, $La(2OHCin)_3$ (blue), lanthanum 3-hydroxy cinnamate, $La(3OHCin)_3$ (green) and lanthanum 4-hydroxy cinnamate, $La(4OHCin)_3$ (red), at 600 ppm and pH 5.5.

Table 5 presents the observed shifts found for each solution of lanthanum 2, 3, and 4-hydroxy cinnamate at a concentration of 400 ppm in a solution of pH 5.5 in 0.01 M NaCl. These data clearly indicate that, the resonance shifts to higher frequencies and the peak width at half height increased in going from $La(4OHCin)_3$ to $La(2OHCin)_3$. The shift in NMR frequency signifies a change in the lanthanum environment possibly brought about by differences in the coordination. The changing width could indicate an increasing number of species and possible exchange between these. Being a quadrupolar nucleus, the width could also indicate an increasingly asymmetric environment. This

speciation behaviour was further investigated using ESMS as discussed below.

Table 5. NMR shifts and ½ widths corresponding to each rare earth cinnamate.

Test Solution	NMR Shift (ppm)	½ Width (Hz)
$LaCl_3$ Reference in D_2O	4.9	179
$La(2OHCin)_3$	16.4	630
$La(3OHCin)_3$	12.5	500
$La(4OHCin)_3$	9.8	470

ESMS measures the mass-to-charge ratio of charged particles. It has been a valuable analytical technique to determine the mass of particles and the elemental composition of a sample in our previous work [15]. The behaviour of the chemical equilibrium will change when there are changes to the reaction conditions, for example a change in the concentration, and therefore a change in the mass-to-charge ratio of the charged species is expected to be observed. Table 6 presents a summary of the rare earth complex species that are expected in the solutions investigated here. Each species containing rare earth metal and/or chloride ions will appear with a particular isotope pattern, these clusters found in the mass spectra, in ESI Figures S1−S5, have been supported by simulated mass spectra and can be found in ESI Figure S6 to S14. Additionally, all reported peaks are the main peak of the associated cluster.

ESI Figures S1 to S5 show, the electrospray mass spectrum obtained for 600 ppm $La(xOH\text{-}Cin)_3$ and $RE(4OHCin)_3$ (RE = Ce, Pr) at pH 5.5. This data demonstrates the change in the mass-to-charge ratio of the species present according to the expected species in Table 6, and also shows that not all inhibitors have the same species present under the given conditions.

Table 6. Species expected in the electrospray mass spectrometry analysis.

Mass	Species	Mass	Species	Mass	Species
281	$[LaCl_4]^-$	282	$[CeCl_4]^-$	283	$[PrCl_4]^-$
407	$[LaLCl_3]^-$	408	$[CeLCl_3]^-$	409	$[PrLCl_3]^-$
535	$[LaL_2Cl_2]^-$	536	$[CeL_2Cl_2]^-$	537	$[PrL_2Cl_2]^-$
663	$[LaL_3Cl]^-$	664	$[CeL_3Cl]^-$	665	$[PrL_3Cl]^-$
791	$[LaL_4]^-$	792	$[CeL_4]^-$	793	$[PrL_4]^-$

Previous work published for the speciation work on $La(4OHCin)_3$ suggested the presence of species as listed in Table 6 (given the mass-to-charge ratios) in varying amounts depends on environmental conditions. An equilibrium between these species was postulated as shown in Equation (1). It was found that the concentration and pH condition was linked to the species present in solution (also supported by NMR spectroscopy). The highest inhibition efficiency observed from potentiodynamic polarisation correlated with the speciation tending towards the right of this equilibrium. This suggests that when species such as $[LaL_3Cl]^-$ and $[LaL_4]^-$ (L = xOHCin) were present, the observed inhibition was greater than when they were absent.

$$[LaCl_4]^- \rightleftharpoons [LaCl_3L]^- \rightleftharpoons [LaCl_2L_2]^- \rightleftharpoons [LaClL_3]^- \rightleftharpoons [LaL_4]^- \quad (1)$$

It was found from the spectrum of $La(2OHCin)_3$ (ESI Figure S4) that the majority of the species present at this particular concentration and solution pH is of lower molecular weight, and consists mainly of species that lie to the left of the equilibrium reaction (Equation 1). In particular and worth noting is the low concentration of the $[LaL_4]^-$ species at 791 mass units. Some of the low molecular weight species present in the spectrum have been attributed to species containing lanthanum and hydroxides and may include species such as $LaL_2(OH)_3(H_2O)_6Cl]^{3-}$, $[LaL_2(OH)_3(H_2O)_6Cl_2]^{4-}$ and $[LaL_2(OH)_3(H_2O)_6Cl_3]^{4-}$. These species not being prevalent in the electrospray mass spectrum of $La(4OHCin)_3$.

The electrospray mass spectrum obtained for $La(3OHCin)_3$ (ESI Figure S3) also shows a number of different species, not unlike the $La(2OHCin)_3$ spectrum. However, the apparent concentrations of these species were more evenly distributed along with the high mass-to-charge ratios of species such as $[LaL_3Cl]^-$ and $[LaL_4]^-$ found in the $La(4OHCin)_3$ spectrum.

As can be seen from the mass spectrum obtained for $Pr(4OHCin)_3$ (Figure 6), it appears similar to that found for $La(4OHCin)_3$ from previous studies. In particular, the peak at 793 mass units is representative of $[PrL_4]^-$ which appears to be the species contributing to the best inhibition seen for mild steel.

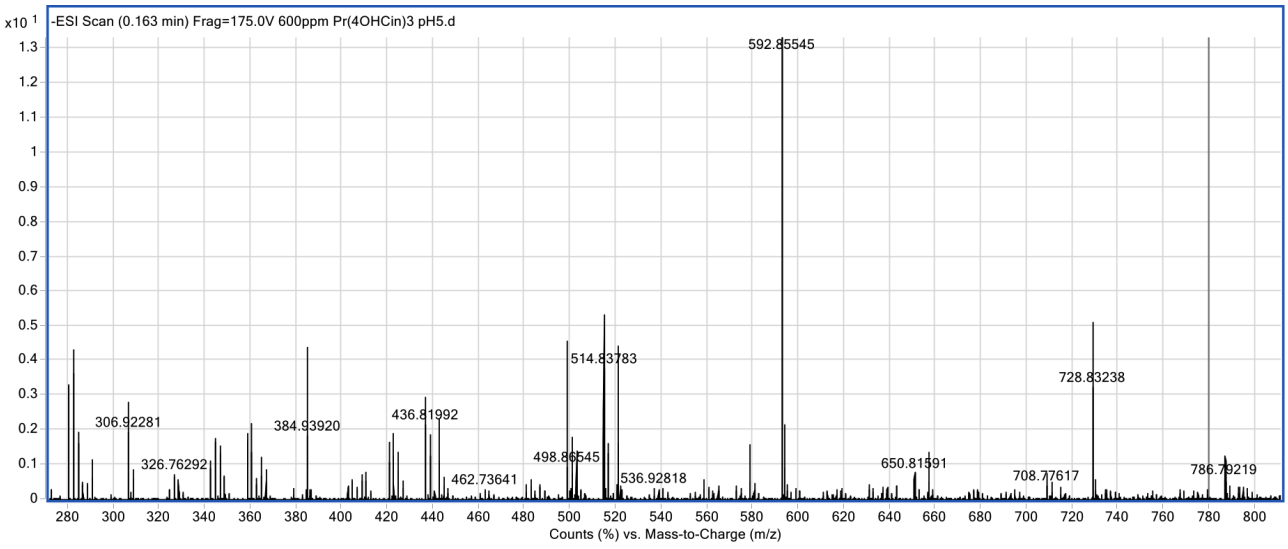

Figure 6. Mass spectrum of praseodymium 4-hydroxy cinnamate ($Pr(4OHCin)_3$) at 600 ppm in 0.01 M NaCl solution at pH 5.5.

The spectrum collected for $Ce(4OHCin)_3$ (ESI Figure S1) appears to be very different from the other compounds; there are fewer species present in solution, which may indicate that the solution equilibria for this inhibitor are quite different. Worth noting at this point is that the solubility of the $Ce(4OHCin)_3$ is high in comparison with the other compounds.

3.3. Hypothesised mechanism of action of inhibitors of steel

We have previously discussed the $La(4OHCin)_3$ inhibition behaviour in the context of the interaction on the metal surface[13,14,15], where a bimetallic film involving the lanthanum complex and the underlying iron from the steel surface forms, and in turn reduces the rate of further metal dissolution at these sites. However, the corrosion is not completely inhibited and some level of corrosion still occurs, leading to changes in the local pH. This change in pH, in particular at the cathodic sites, leads to the hydrolysis of the $La(4OHCin)_3$ species forming a dynamic mixture of lanthanum hydroxide, iron oxide and bimetallic species.

This mechanism was supported in previous work using Attenuated Total Reflectance Fourier Transform Infrared (ATR-FTIR) vibrational spectroscopy [16,17]. This technique proved to be a valuable tool in developing an understanding of the nature of the species on the inhibited surface [22], allowing the examination of the inhibiting complexes attached to the surface without the need to remove the film.

In the current study, the reduction in the observed I_{corr} from $La(2OHCin)_3$, $Ce(4OHCin)_3$, $La(3OHCin)_3$, $Pr(4OHCin)_3$ to $La(4OHCin)_3$ may be related to an increase in the availability of hydroxyl groups as donors in bonding to neighbouring molecules on the steel surface, which therefore influences the bimetallic complex formed.

Based on the schematic protective film shown in Figure 7, the orientations of the hydroxyl group are important for further interactions beyond the initial layer of bimetallic complex. As described in previous reports, the terminal hydroxyl group from the 4-hydroxycinnamate ligand (Fig 7a) is capable of intermolecular interactions (through hydrogen bonding) to nearby molecules of the inhibitor. These effectively increase the thickness of the protective film and result in the precipitation of the rare earth metal hydroxide and iron oxides/hydroxides onto the surface due to local changes in the pH. With this ongoing process, it would be reasonable to suggest that the protective film could ultimately lead to a more uniform surface coverage [23].

For the $La(3OHCin)_3$, the mechanism of film formation could be very similar in that the hydroxyl group is positioned in a geometry that is accessible to promote further interactions either with the La ion or the underlying substrate, as shown in Figure 7b. Whilst for the $La(2OHCin)_3$ inhibitor, the *ortho*-substitution causes the hydroxyl groups to be shielded by the aromatic ring (Fig 7c), sterically hindering further interactions, and therefore eliminating the possibility of forming a multilayer surface film that might be possible for either the $La(3OHCin)_3$ and the $La(4OHCin)_3$ inhibitors.

In the case of $Pr(4OHCin)_3$ and $Ce(4OHCin)_3$, the hydroxy group is in the *para*-position, as in the $La(4OHCin)_3$, and therefore capable of further intermolecular interactions. This would explain the excellent inhibition shown by the $Pr(4OHCin)_3$. In contrast, $Ce(4OHCin)_3$ does not show good inhibiting properties consistent with the differences in speciation observed in the electrospray mass spectroscopy. Interestingly, we observed that the solubility of the cerium compounds is generally significantly higher than the praseodymium and lanthanum analogues (for example $Ce(4OHCin)_3$ at 1000 ppm readily dissolves in the sodium chloride solution whereas $Pr(4OHCin)_3$ and $La(4OHCin)_3$ compounds are difficult to dissolve beyond 600 ppm at neutral pH). This is contrary to the solubility data in water for $La(4OHCin)_3$ and $Ce(4OHCin)_3$ which were found to be 961 ppm and 673 ppm, respectively, where the lanthanum compound was marginally more soluble than the cerium derivative [24]. The difference in solubility is often related to the size of the rare earth metal cation,

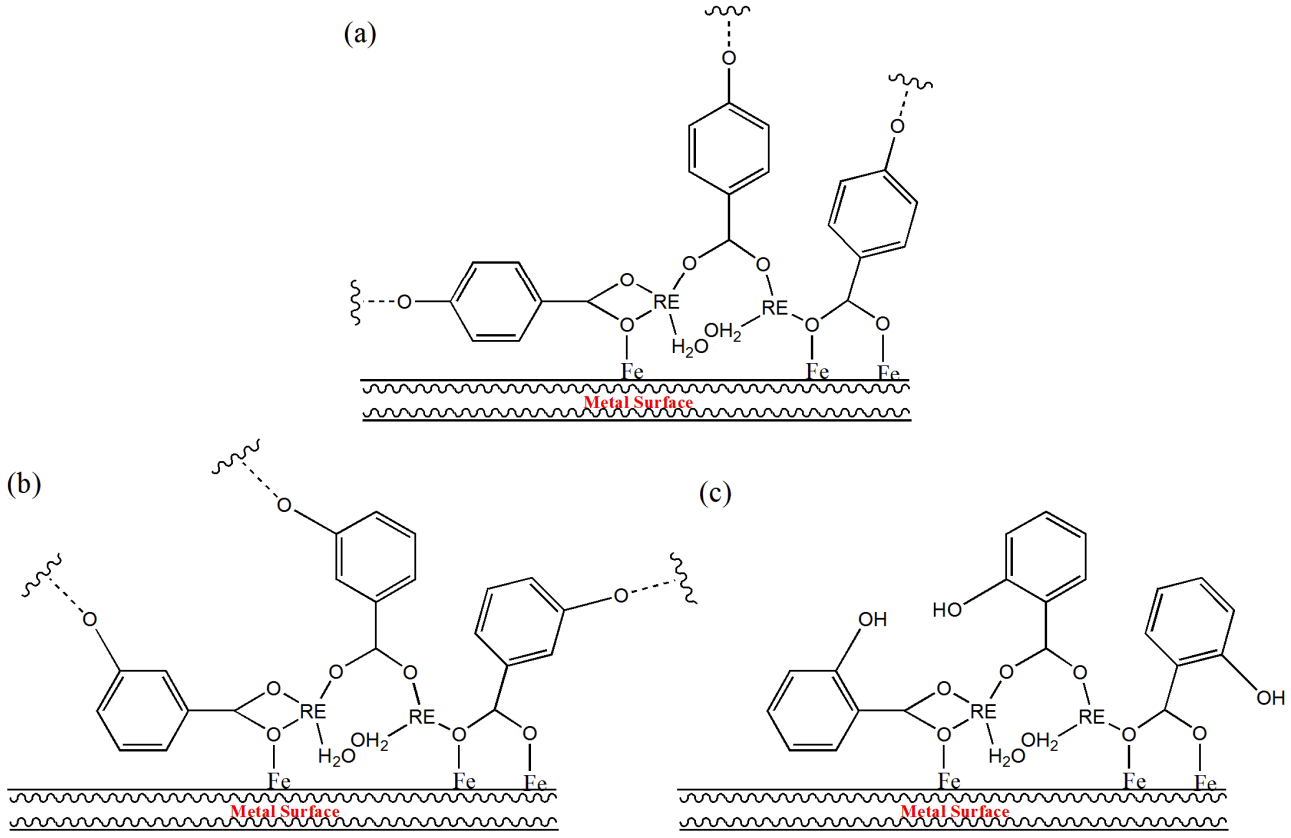

Figure 7. A schematic hypothesised mechanism of action for the protection of a steel substrate using the inhibitor (a) RE(4OHCin)$_3$ where RE = La, Ce and Pr, (b) La(3OHCin)$_3$ and (c) La(2OHCin)$_3$.

however given that $La^{3+} > Ce^{3+} > Pr^{3+}$, this cannot explain our observations here. Furthermore, the X-ray powder diffraction patterns show that the compounds are all iso-structural having similar d-spacings and intensities and that the isomorphous RE(4OHCin)$_3$ have very similar ν(OH) absorptions [18]. Additional information on the solid state compositions and structures of the rare earth n-hydroxycinnamates can be found in the ESI. The other differences amongst these rare earth metal cations is the existence of two redox states for Ce(III/IV) compared with Pr(III) and La(III). It has been previously shown that Ce(III) can readily oxidise from the Ce^{3+} to Ce^{4+} in the presence of oxygen and water with some ligands [25]. The presence of this redox couple may result in the formation of different complex species that would not otherwise be seen in the lanthanum and/or praseodymium systems. This possibility is supported by the difference seen in the mass spectrum of the cerium compound, ESI Figure S1, compared to lanthanum 4-hydroxycinnamate (ESI Fig S5). However, further work is required to fully understand the complexation in this system, as we are unable to assign the spectrum obtained in this case. Thus the mechanism of inhibition for the Ce(4OHCin)$_3$ complex differs from that of La(4OHCin)$_3$ and Pr(4OHCin)$_3$ due to both the solubility and the oxidation states (Ce^{3+} to Ce^{4+}). In our previous work, we have shown that the nature of the metal – ligand complexes in solution are critical for the corrosion inhibition efficiency; in particular the presence of species such as $[LnL_4]^-$ and $[LnL_3Cl]^-$. The absence of these in the case of Ce(4OHCin)$_3$ may contribute to the poorer inhibition. Thus the model proposed in Figure 6 may not

apply to $Ce(4OHCin)_3$.

4. Conclusion

The present work has focussed on understanding the influence of the rare earth metal cations and the hydroxycinnamate structure on the corrosion inhibition properties for the rare earth cinnamate compounds. Consistent with previous work, the $La(4OHCin)_3$ performed best with $Pr(4OHCin)_3$ and $La(3OHCin)_3$ showing near comparable inhibition efficiencies using potentiodynamic polarisation measurements. On the other hand, the $Ce(4OHCin)_3$ showed poorer inhibition properties correlating with the markedly different species observed in the mass spectrum. We hypothesise that this is related in some way to increased solubility and the two accessible oxidation states for cerium. Furthermore, the availability of the phenol group of the rare earth hydroxycinnamates for intermolecular interactions appears to be imperative for good corrosion inhibition as demonstrated by the poorer performance of $La(2OHCin)_3$ with the phenol group shielded by the phenyl-ring.

Acknowledgements

We thank the ARC Centre of Excellence for Electromaterials and the SRC for Green Chemistry for funding resources in this study. We also gratefully acknowledge the invaluable discussions with Dr. Craig Forsyth.

Conflict of interest

All authors declare no conflicts of interest in this paper.

References

1. McCafferty E (1979) Inhibition of the Crevice Corrosion of Iron in Chloride Solutions by Chromate. *J Electrochem Soc* 126: 385–390.
2. Maji KD, Singh I (1982) Studies on the effect of sulphide ions on the inhibition efficiency of chromate on mild steel using radio—tracer technique. *Anti-Corros Method M* 29: 8–14.
3. McCafferty E (1989) Thermodynamic aspects of the crevice corrosion of iron in chromate/chloride solutions. *Corros Sci* 29: 391–401.
4. Mercer AD (1990) Chemical Inhibitors for Corrosion Control B; Clubley G, editor: Royal Society of Chemistry Cambridge UK.
5. Jones DA (1996) Principles and Prevention of Corrosion: Prentice hall.
6. Roberge PR (2000) Handbook of Corrosion Engineering. New Jersey: McGraw Hill.
7. Sinko J (2001) Challenges of chromate inhibitor pigments replacement in organic coatings. *Prog Org Coat* 42: 267–282.
8. Monticelli C, Frignani A, Trabanelli G (2002) Corrosion inhibition of steel in chloride-containing alkaline solutions. *J Appl Electrochem* 32: 527–535.
9. Grundmeier G, Schmidt W, Stratmann M (2000) Corrosion protection by organic coatings: electrochemical mechanism and novel methods of investigation. *Electrochim Acta* 45:

2515–2533.
10. Blin F, Koutsoukos P, Klepetsianis P, et al. (2007) The corrosion inhibition mechanism of new rare earth cinnamate compounds—Electrochemical studies. *Electrochim Acta* 52: 6212–6220.
11. Blin F, Leary SG, Wilson K, et al. (2004) Corrosion Mitigation of Mild Steel by New Rare Earth Cinnamate Compounds. *J Appl Electrochem* 34: 591–599.
12. Deacon GB, Forsyth M, Junk P, et al. (2008) From chromates to rare earth carboxylates: a greener take on corrosion inhibition. *Chemistry Australia* 75: 18–21.
13. Forsyth M, Seter M, Hinton B, et al. (2011) New 'Green' Corrosion Inhibitors Based on Rare Earth Compounds. *Aust J Chem* 64:812–819.
14. Catubig R, Seter M, Neil W, et al. (2011) Effects of Corrosion Inhibiting Pigment Lanthanum 4-Hydroxy Cinnamate on the Filiform Corrosion of Coated Steel. *J Electrochem Soc* 158: C353–C358.
15. Seter M, Hinton B, Forsyth M (2012) Understanding Speciation of Lanthanum 4-Hydroxy Cinnamate and its Impact on the Corrosion Inhibition Mechanism for AS1020 Steel. *J Electrochem Soc* 159: C181–C189.
16. Blin F, Leary SG, Deacon GB, et al. (2006) The nature of the surface film on steel treated with cerium and lanthanum cinnamate based corrosion inhibitors. *Corros Sci* 48: 404–419.
17. Forsyth M, Forsyth CM, Wilson K, et al. (2002) ATR characterisation of synergistic corrosion inhibition of mild steel surfaces by cerium salicylate. *Corros Sci* 44: 2651–2656.
18. Deacon GB, Forsyth M, Junk PC, et al. (2009) Synthesis and Characterisation of Rare Earth Complexes Supported by para-Substituted Cinnamate Ligands. *Z Anorg Allg Chem* 635: 833–839.
19. Reuben J, Fiat D (1969) Nuclear Magnetic Resonance Studies of Solutions of the Rare-Earth Ions and Their Complexes. IV. Concentration and Temperature Dependence of the Oxygen-17 Transverse Relaxation in Aqueous Solutions. *J Chem Phys* 51: 4918–4927.
20. Aime S, Fasano M, Terreno E (1998) Lanthanide(III) chelates for NMR biomedical applications. *Chem Soc Rev* 27: 19–29.
21. Bryant RG (1983) The NMR time scale. *J Chem Educ* 60: 933–935.
22. Pandey A, Murty NSS, Patel SM (2000) Application of infrared spectroscopy in the study of corrosion products. *Process Contr Qual* 11: 363–368.
23. Deacon GB, Forsyth CM, Behrsing T, et al. (2002) Heterometallic CeIII-FeIII-salicylate networks: models for corrosion mitigation of steel surfaces by the Green inhibitor, Ce(salicylate)3. *Chem Commun* 23: 2820–2821.
24 Leary SG. Green corrosion inhibitors for coating applications. Ph.D. Thesis, Monash University, 2005.
25 Behrsing T, Bond AM, Deacon GB, et al. (2003) Cerium acetylacetonates—new aspects, including the lamellar clathrate [Ce(acac)4]·10H2O. *Inorg Chim Acta* 352: 229–237